

# UCSF

## UC San Francisco Previously Published Works

### Title

Control of an Unusual Photo-Claisen Rearrangement in Coumarin Caged Tamoxifen through an Extended Spacer

### Permalink

<https://escholarship.org/uc/item/73n2z62r>

### Journal

ACS Chemical Biology, 12(4)

### ISSN

1554-8929

### Authors

Wong, Pamela T  
Roberts, Edward W  
Tang, Shengzhuang  
et al.

### Publication Date

2017-04-21

### DOI

10.1021/acscchembio.6b00999

Peer reviewed

# Control of an Unusual Photo-Claisen Rearrangement in Coumarin Caged Tamoxifen through an Extended Spacer

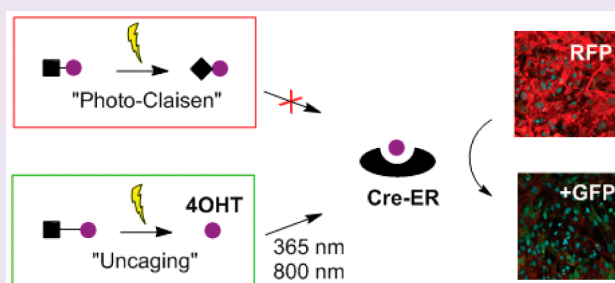
Pamela T. Wong,<sup>†,‡,||</sup> Edward W. Roberts,<sup>§,||</sup> Shengzhuang Tang,<sup>†,‡</sup> Jhindan Mukherjee,<sup>†,‡</sup> Jayme Cannon,<sup>†,‡</sup> Alyssa J. Nip,<sup>§</sup> Kaitlin Corbin,<sup>§</sup> Matthew F. Krummel,<sup>\*,§</sup> and Seok Ki Choi<sup>\*,†,‡,§</sup>

<sup>†</sup>Michigan Nanotechnology Institute for Medicine and Biological Sciences and <sup>‡</sup>Department of Internal Medicine, University of Michigan Medical School, Ann Arbor, Michigan 48109, United States

<sup>§</sup>Department of Pathology, University of California, San Francisco, 513 Parnassus Ave, HSW512, San Francisco, California 94143, United States

## S Supporting Information

**ABSTRACT:** The use of coumarin caged molecules has been well documented in numerous photocaging applications including for the spatiotemporal control of Cre-estrogen receptor (Cre-ERT2) recombinase activity. In this article, we report that 4-hydroxytamoxifen (4OHT) caged with coumarin *via* a conventional ether linkage led to an unexpected photo-Claisen rearrangement which significantly competed with the release of free 4OHT. The basis for this unwanted reaction appears to be related to the coumarin structure and its radical-based mechanism of uncaging, as it did not occur in *ortho*-nitrobenzyl (ONB) caged 4OHT that was otherwise linked in the same manner. In an effort to perform design optimization, we introduced a self-immolative linker longer than the ether linkage and identified an optimal linker which allowed rapid 4OHT release by both single-photon and two-photon absorption mechanisms. The ability of this construct to actively control Cre-ERT2 mediated gene modifications was investigated in mouse embryonic fibroblasts (MEFs) in which the expression of a green fluorescent protein (GFP) reporter dependent gene recombination was controlled by 4OHT release and measured by confocal fluorescence microscopy and flow cytometry. In summary, we report the implications of this photo-Claisen rearrangement in coumarin caged compounds and demonstrate a rational linker strategy for addressing this unwanted side reaction.



The application of photocaging technology<sup>1–3</sup> has yielded numerous novel photoprobes that have enabled the active control of molecular activities and cellular processes by light. The fundamental concept behind these strategies is the temporary inactivation of a biologically active molecule through the covalent attachment of a photocleavable cage molecule until the caged molecule is reactivated by light exposure.<sup>2</sup> Several types of cage molecules, each distinct in their structural and photochemical properties,<sup>4–6</sup> have been reported, including *ortho*-nitrobenzene (ONB),<sup>1,7,8</sup> coumarin,<sup>9,10</sup> nitrobenzofuran,<sup>11</sup> and quinoline<sup>12</sup> chromophores. The contributions of their applications have been well documented in numerous fields ranging from ion channels<sup>1,13</sup> and enzymes<sup>14,15</sup> to gene expression,<sup>16</sup> photopharmacology,<sup>17,18</sup> and controlled drug transport or delivery.<sup>19–21</sup>

Recently, a number of laboratories,<sup>22–24</sup> including ours,<sup>25,26</sup> have reported on caged forms of ligands for the estrogen receptor (ER), such as tamoxifen (TAM),<sup>26</sup> 4-hydroxytamoxifen (4OHT),<sup>25,27</sup> and their homologues,<sup>22–24</sup> and have validated their ability to control light-inducible reporter gene modifications in optogenetic models.<sup>23,28</sup> In our studies,<sup>25,26</sup> we used transgenic mouse embryonic fibroblasts (MEFs) with a reporter cassette (mTmG<sup>29</sup>) which contains a gene for red

fluorescent protein (RFP) TdTomato flanked by loxP sites (Figure 1). These MEFs also constitutively express Cre recombinase fused to a modified ER that has a reduced affinity for native estrogen (UbcCre-ERT2<sup>30</sup>). In the absence of ER ligand, Cre-ERT2 recombinase remains bound to cytoplasmic Hsp70, and the MEFs constitutively express RFP. However, upon binding uncaged ligand, Cre-ERT2 dissociates from Hsp70 and is translocated to the nucleus where it can then excise the loxP-flanked gene for TdTomato from the mTmG<sup>29</sup> reporter construct, resulting in the expression of a membrane-bound green fluorescence protein (GFP). We reported that 1 ONB-L<sub>1</sub>-4OHT, which is highly water-soluble ( $\geq 20$  mg mL<sup>-1</sup>) and cell permeable, has the ability to induce reporter expression with a spatial resolution sufficient for selectively marking cells.<sup>25</sup>

The uncaging efficiency of tamoxifen caged compounds reported in existing Cre-ER models is based on a single-photon mechanism of activation which typically occurs by absorption of light in the UV range. However, the efficiency of two-photon mechanisms of activation which use longer wavelength, near-

Received: November 9, 2016

Accepted: February 13, 2017

Published: February 13, 2017

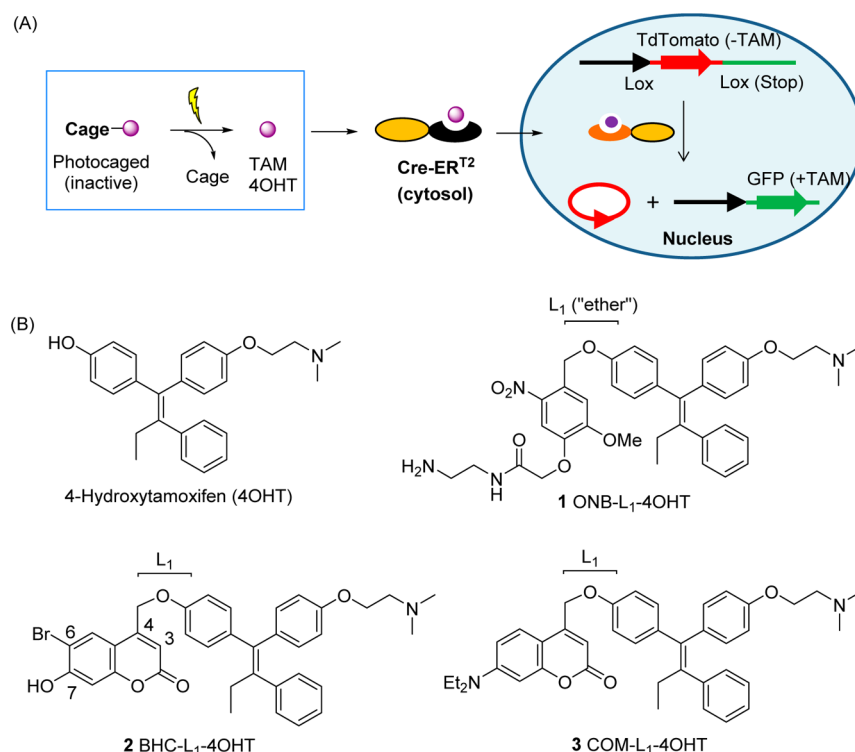


**Figure 1.** Photocontrol of Cre-ER mediated GFP expression. (A) Schematic for light-triggered activation of photocaged tamoxifen (TAM) or 4-hydroxytamoxifen (4OHT), and the control of reporter gene expression mediated by the Cre recombinase-estrogen receptor (ER) fusion protein. (B) Structures of 4OHT and its caged compounds including a previously reported **1** ONB- $L_1$ -4OHT,<sup>25</sup> and two new compounds **2** BHC- $L_1$ -4OHT and **3** COM- $L_1$ -4OHT, each caged with BHC or COM through an ether linkage ( $L_1$ ), respectively. Abbreviations: ONB = *ortho*-nitrobenzyl; BHC = 6-bromo-7-hydroxycoumarin-4-methyl; COM = 6-diethylaminocoumarin-4-methyl.

infrared (NIR) light remains mostly unevaluated.<sup>24</sup> Two-photon uncaging of photocaged compounds occurs only on the focal plane with small cross sections of absorption,<sup>6</sup> but it offers significant unique advantages over the single-photon UV activation including the deeper penetration capabilities of NIR light in tissue, as well as reduced light scattering and greater spatial resolution.<sup>6,9</sup> Subsequently, our current efforts focused on the design and validation of new 4OHT caged compounds for their uncaging efficiency by both single- and two-photon mechanisms *in vitro*.

Here, we discuss the light-controlled recombinase activity observed in the two series of 4OHT-caged compounds, the first based on the ONB cage including **1** ONB- $L_1$ -4OHT, and the second based on the coumarin cage which was selected for its susceptibility to one-photon uncaging by UV-visible light (405–420 nm)<sup>7,31,32</sup> as well as for its enhanced cross sections for two-photon uncaging ( $\delta_{\text{uncaging}}/\text{GM} = 0.21\text{--}1.99$ ) compared to ONB ( $\delta_{\text{uncaging}}/\text{GM} = 0.01\text{--}0.23$ ).<sup>6</sup> The importance of linker selection in the design of 4OHT caged compounds was then examined. Despite its important role in conjugation chemistry, the “linkage” or “linker” (linkage + spacer) is generally less prioritized in the design of caged compounds than the cage itself because it has hitherto been thought of as playing no direct role in triggering the uncaging reaction and having no contribution to the wavelength selectivity of the cage. Here, we provide evidence that the use of a standard linker can lead to poor uncaging efficiency, as illustrated by the dramatically reduced uncaging efficiency of a coumarin cage attached directly to the phenolic substrate, 4OHT, through an ether linkage. Specifically, use of this linkage led to the unanticipated occurrence of a photo-Claisen rearrangement<sup>33</sup> as the major

reaction path and thus significantly reduced the efficiency of free drug release. We demonstrate that the occurrence of such undesired reaction is effectively blocked by application of alternative linker chemistry.

## RESULTS AND DISCUSSION

**Synthesis of Coumarin Caged 4OHT via Ether Linkage.** Using a similar linker strategy applied for ONB-based compound **1**,<sup>25</sup> we designed two coumarin caged compounds of 4OHT, **2** BHC- $L_1$ -4OHT, and **3** COM- $L_1$ -4OHT (Figure 1), each by tethering 4OHT (Z and E isomers) at its phenolic moiety to a BHC (6-bromo-7-hydroxycoumarin-4-methyl)<sup>9</sup> or COM (6-diethylaminocoumarin-4-methyl)<sup>7</sup> cage molecule through an ether linkage. The synthesis of **2** and **3** was performed by direct *O*-alkylation of 4OHT with the corresponding coumarinyl-4-methylmethanesulfonate. Each of these caged compounds was obtained with a purity of  $\geq 95\%$  (UPLC) without detectable free 4OHT (Figure S6, Supporting Information). Their structural identity was fully characterized by a combination of standard analytical methods including NMR (<sup>1</sup>H, <sup>13</sup>C) spectroscopy (Figures S1–S5), mass spectrometry, and UV-vis spectrophotometry (Supporting Information). The exact molecular masses of **2** and **3** are in good agreement with the experimental values measured by high resolution mass spectrometry (HRMS): calcd for **2** C<sub>36</sub>H<sub>34</sub>BrNO<sub>5</sub> [M + H]<sup>+</sup>, 640.1693; found, 640.1711; calcd for **3** C<sub>40</sub>H<sub>44</sub>N<sub>2</sub>O<sub>4</sub> [M + H]<sup>+</sup>, 617.3374; found, 617.3373.

**Unusual Release Kinetics of **2** and **3**.** We investigated the efficiency of light-controlled release of 4OHT from **2** by exposure to long wavelength UVA light (max intensity at 365 nm; Figure 2). After photolysis, the exposed solutions were

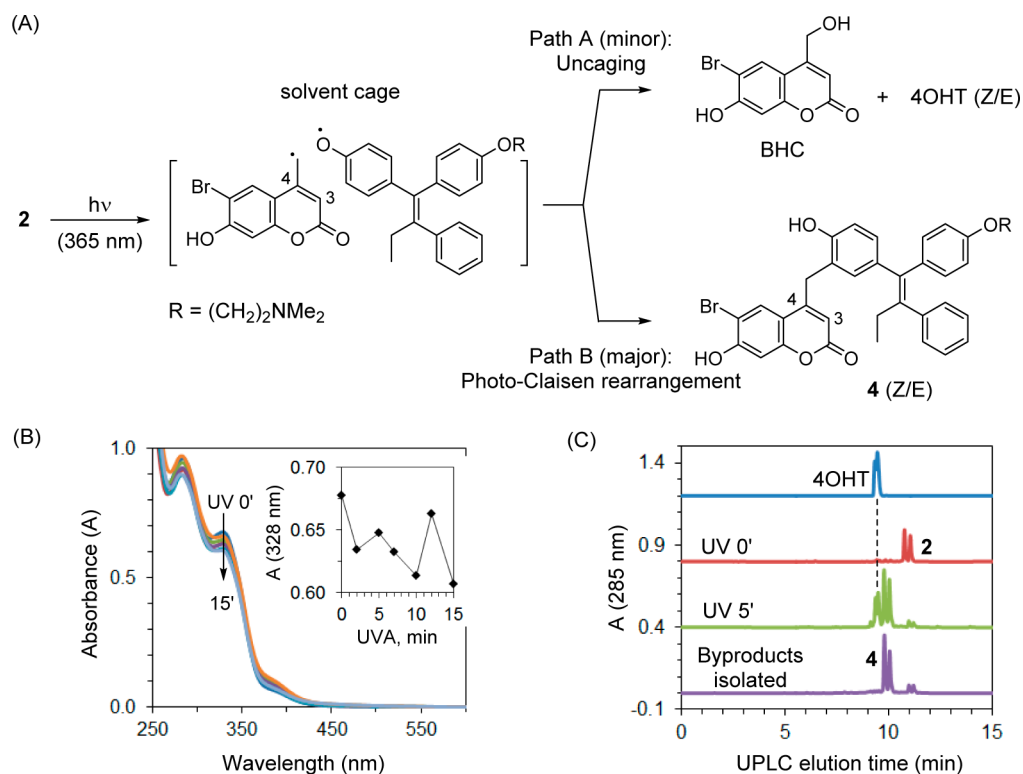


**Figure 2.** Mechanism of photo-Claisen rearrangement. (A) Two competing reaction paths of 2 BHC-L<sub>1</sub>-4OHT (Z and E isomers) that occur in response to light (365 nm); path A leading to free 4OHT and path B toward the formation of a major byproduct 4 (Z/E isomers) *via* photo-Claisen rearrangement. (B) Overlaid UV-vis spectra. Inset (B): a plot of absorbance at 328 nm against UV exposure time. (C) UPLC traces acquired for references and photolyzed 2 (78  $\mu$ M in 20% (v/v) aqueous methanol).

analyzed by thin layer chromatography (TLC; Figure S7), which demonstrated the rapid disappearance of 2 with the concomitant growth of a broad spot that migrated as far as the 4OHT reference molecule. However, while subsequent quantitative analysis performed by ultrahigh performance liquid chromatography (UPLC) also indicated the release of 4OHT, it revealed that it was only as a minor fraction of the total products ( $\Phi_{4\text{OHT}} = 0.09$ ). The majority of the product consisted of a pair of closely running, unknown products ( $t_r = 10$  min) with the  $\sim 1:2$  AUC (area under curve) ratio of the total of these two peaks relative to the 4OHT peak (Figure 2C). The unknown products were isolated by flash column chromatography, and their structural identity was assigned as 4 (Z/E isomers) based on the combination of data from <sup>1</sup>H NMR spectroscopy and LC-MS mass spectrometry. Thus, analysis of the LC-MS data indicated no change in the molecular mass ( $[M + H]^+ = 640.1680$ ) compared to the parent caged molecule 2 (Figure S8). The <sup>1</sup>H NMR spectral analysis shows alterations broadly in 4OHT and BHC signals (Figure S9), in particular, in those from C-3 and C-4 protons which are assigned in reference to C3- or C4-substituted coumarin compounds (Table S1).<sup>34,35</sup> On the basis of these data, we believe that 4 was formed *via* the photo-Claisen rearrangement<sup>33</sup> of 2 as proposed in Figure 2 with a quantum efficiency ( $\Phi_{\text{Photo-Claisen}} = 0.22$ ) greater than that of 4OHT release ( $\Phi_{4\text{OHT}} = 0.09$ ). The occurrence of these unexpected products from 2 is, in retrospect, explained by its [3,3] bond framework, which is composed of an allyl (BHC)-to-aryl (4OHT) ether, a unique structural feature required for the occurrence of photo-Claisen rearrangement.<sup>33,36</sup>

However, it is noteworthy that 1 ONB-L<sub>1</sub>-4OHT, which similarly meets a structural requirement by having an allyl (ONB)-to-aryl ether framework, did not show such byproduct formation but, instead, released 4OHT predominantly as a single product ( $\Phi_{4\text{OHT}} = 0.13$ ) in our earlier study.<sup>25</sup> We further investigated whether such differences in the product distribution between 1 and 2 are specifically inherent to the coumarin cage by performing the release study with 3 COM-L<sub>1</sub>-4OHT, a close analogue of 2. Its product distribution was consistent with that of 2, demonstrating 4OHT release as a minor fraction of the products ( $\Phi_{4\text{OHT}} = 0.03$ ) along with a larger fraction of isomeric products ( $\Phi_{\text{Photo-Claisen}} = 0.05$ ) which are identical to 3 in their molecular masses as characterized by LC-MS mass spectrometry ( $[M + H]^+ = 617.3369$ ; Figure S10). These results suggest that photo-Claisen products might occur selectively for coumarin caged molecules, while the differences observed in quantum efficiency between BHC and COM might be determined by the nature of the aromatic ring substituents on each coumarin cage.

Use of coumarin caged molecules has gained strong popularity due to their high quantum efficiency of uncaging and broad applicability to various functional substrates.<sup>6</sup> However, the photochemical properties of the coumarin cage which are responsible for leading to a dead-end side product instead of the desired uncaging reaction have rarely been noted except for the recent identification of the photoisomerization of BHC caged cysteine-containing peptides (C<sub>4</sub>-CH<sub>2</sub>S to C<sub>3</sub>-S) by Distefano *et al.*<sup>37</sup> and Hagen *et al.*,<sup>31</sup> and the photo-rearrangement of 4-coumarinylmethyl phenyl ethers by Hagen and co-workers.<sup>34</sup> Thus, our study offers strong evidence for the broader occurrence of photorearrangement specifically in

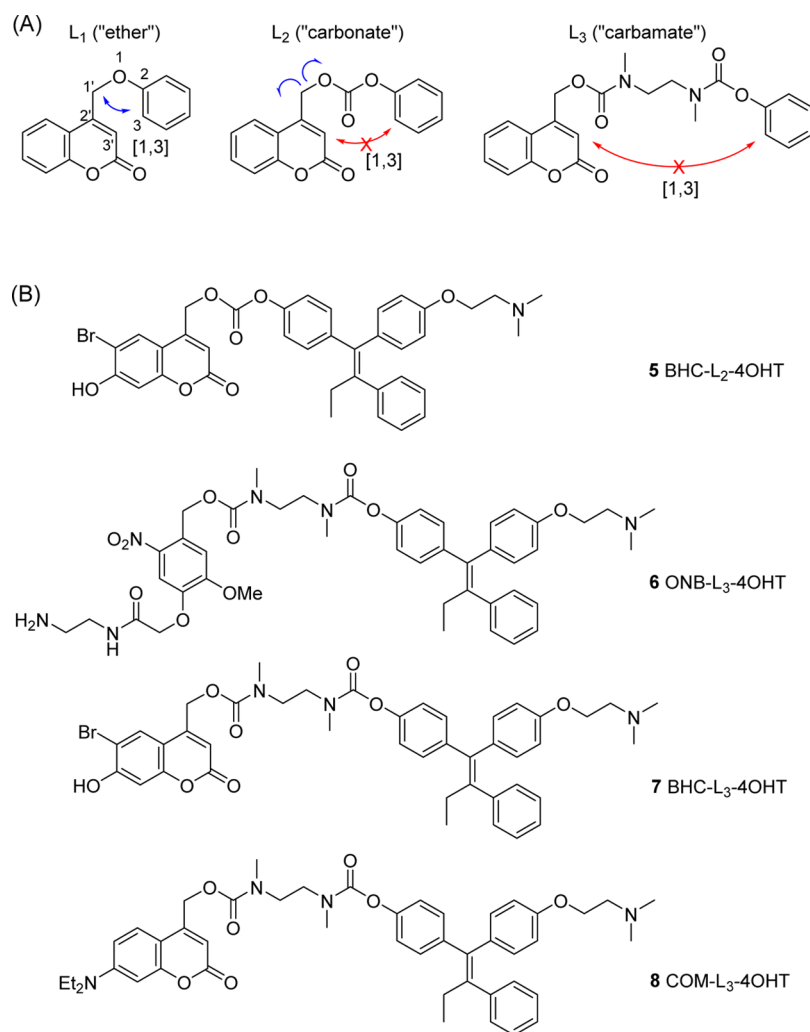


**Figure 3.** Design of extended spacers. (A) Release mechanism of extended linkers for coumarin-caged phenolic compounds in which photo-Claisen [1,3] rearrangement is forbidden due to a lack of close proximity, and self-immolation occurs instead. (B) Two linker classes used in coumarin or ONB-caged 4OHT compounds 5–8. 4OHT is tethered to each cage molecule through a carbonate ( $L_2$ ) or carbamate ( $L_3$ ) linker.

the class of coumarin caged compounds designed with a direct ether linkage to a target molecule. It also shows that this rearrangement reaction significantly reduces the uncaging efficiency and suggests the need for improving the design features in coumarin caged compounds.

**Coumarin Caged 4OHT via Extended Linker.** We hypothesize that the selective occurrence of photo-Claisen rearrangement in the ether-linked coumarin caged compounds is attributable to the radical mechanism of C–O bond cleavage in combination with physical proximity between the two radical species formed that allows recombination before they escape from their solvent cage (Figure 2).<sup>33</sup> To circumvent such proximity-promoted photo-Claisen rearrangement, we focused our design approach on extension of the linkage through either a self-immolative<sup>38,39</sup> carbonate ( $L_2$ ) or carbamate linker ( $L_3$ ) that provides an effective physical barrier to separate two radical species to be formed far enough for their escape and release. Use of these extended linkers was previously reported for photocaged compounds including BHC-caged ceramides (carbonate linkage),<sup>40</sup> ONB-caged rapamycin (carbonate),<sup>15</sup> and ONB-caged 4OHT (carbamate).<sup>25</sup> Application of these two linkers led to the synthesis of two classes of caged compounds 5–8 as shown in Figure 3: (i) the carbonate-linked

5 BHC- $L_2$ -4OHT; (ii) the carbamate-linked 6 ONB- $L_3$ -4OHT,<sup>25</sup> 7 BHC- $L_3$ -4OHT, and 8 COM- $L_3$ -4OHT. Compound homogeneity was  $\geq 95\%$  for each of these caged compounds as determined by UPLC analysis (Figure S6), and their structural identity was fully supported by data collected by standard analytical methods as described above (Supporting Information).

**Release Kinetics of Extended Linkers.** We next evaluated the release kinetics of 5 BHC- $L_2$ -4OHT (125  $\mu\text{M}$  in 20% (v/v) aqueous methanol) upon exposure to UVA light (Figure S11). UPLC analysis of the photolyzed solution indicated rapid release of 4OHT (73% after 2 min). However, its 4OHT release was also observed in the dark (9% at 2 h), pointing to the hydrolytic instability of the carbonate linkage in 5 in the aqueous solution.

We then investigated the release kinetics of the carbamate-linked caged compounds 7 and 8. Exposure to UVA light triggered the release of free 4OHT through formation of its carbamate derivative 9 (Figure 4, Figure S12). UPLC analysis indicates that drug release occurred in an exposure time-dependent manner and resulted in  $\sim 70\%$  release of 4OHT and its direct precursor 9 after exposure for 5 min (7) and 10 min (8). 4OHT release was also confirmed by LC-MS mass



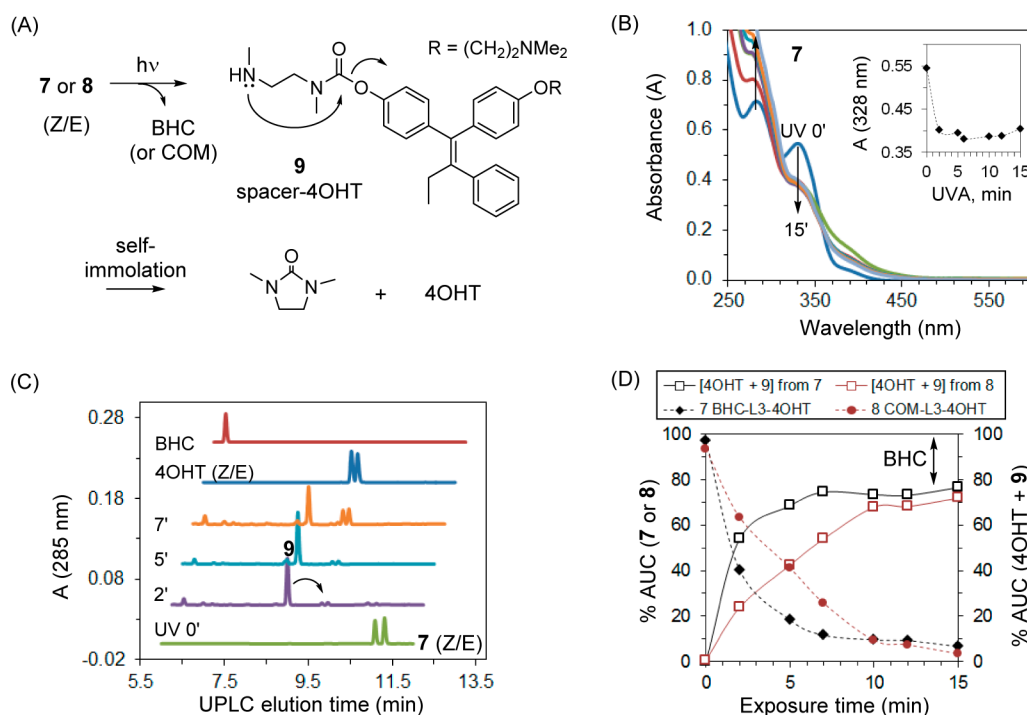


**Figure 4.** Release kinetics of coumarin-caged 4OHT. (A) A mechanism for the photoactivation of 7 BHC-L<sub>3</sub>-4OHT and 8 COM-L<sub>3</sub>-4OHT that involves cleavage to 9 spacer-4OHT, and subsequent self-immolative cyclization of 9, resulting in release of 4OHT. (B, C) UV-vis spectra and UPLC traces obtained after the photolysis of 7 (110 μM, 20% (v/v) aqueous methanol) as a function of exposure time. (D) A plot of the photochemical release kinetics of products (4OHT + 9; %AUC from UPLC traces), each from 7 or 8, respectively.

spectrometric analysis, which showed the appearance of a single peak corresponding to free 4OHT ( $[M + H]^+ = 388.2269$ ; Figure S13). Regression analysis of the decay curve of 7 or 8 (% AUC, Figure 4C) over the exposure time suggests that 7 is consumed with a rate constant (first-order decay,  $k$ ) of  $0.343 \text{ min}^{-1}$ , which is faster than that of 8 ( $k = 0.192 \text{ min}^{-1}$ ) at a comparable concentration. The greater decay rate of 7 is positively correlated with its higher rate of 4OHT release (Figure 4D), suggesting that its initial cleavage to 9 which is triggered by light serves as the rate-determining step for the release of a drug. As a consequence, the quantum efficiency of uncaging ( $\Phi_{[4\text{OHT}+9]}$ ) calculated for 7 (0.21) is higher than those of 6 (0.05) and 8 (0.07) as summarized in Table 1. This greater release efficiency suggests an advantage of using 7 over 8 as the more promising probe for two-photon activation and reporter gene expression in cells as discussed below.

In summary, the two extended linker classes investigated here are distinguished not only by the aqueous stability of their linkages but also by their modes of achieving drug release. First, the carbonate linker used in 5 shows excellent photochemical ability to release free 4OHT with a decay rate greater than either of the carbamate-linked compounds, 7 or 8. However, it lacks sufficient chemical stability in aqueous solution, which is needed for precise active control. Such instability is anticipated to be worse in cell media and in *in vivo* environments that contain substantially higher concentrations (mM) of various nucleophilic species such as amino acids, amines, and protein molecules. This insufficient stability of the carbonate linkage as observed in 5 was not noted previously in other caged compounds linked through a carbonate moiety to the ONB<sup>15</sup> or BHC<sup>40</sup> cage, indicating perhaps the involvement of other additional factors such as the steric effect of the substrate molecules themselves. In contrast, the carbamate-linked

**Table 1. Summary of the Photochemical Properties of Caged 4-Hydroxytamoxifen (4OHT) Compounds**

cage-linker (L <sub>n</sub> )-4OHT	linkage	$\lambda_{\text{max}}$ nm ( $\epsilon$ , M <sup>-1</sup> cm <sup>-1</sup> )	$\Phi^a$	
			4OHT	photo- Claisen 4 + 9
1 ONB-L <sub>1</sub> - 4OHT <sup>rel25</sup>	ether	340 (390)	0.13	nd
2 BHC-L <sub>1</sub> - 4OHT	ether	328 (8,787)	0.09	0.22
3 COM-L <sub>1</sub> - 4OHT	ether	394 (11,357)	0.03	0.05
5 BHC-L <sub>2</sub> - 4OHT	carbonate	340 (6,154)	0.11 <sup>b</sup>	nd
6 ONB-L <sub>3</sub> - 4OHT <sup>rel25</sup>	carbamate	340 (317)	nd	0.05
7 BHC-L <sub>3</sub> - 4OHT	carbamate	330 (9,990)	nd	0.21
8 COM-L <sub>3</sub> - 4OHT	carbamate	394 (13,500)	nd	0.07

<sup>a</sup>Single-photon quantum efficiency  $\Phi = [dc/dt]_{\text{initial}}/[q_{\text{np}}(1-10^{-A})]$  where  $q_{\text{np}}$  = photon flux ( $q_{\text{p}}/N_{\text{A}} = 11.65 \times 10^{-8} \text{ mol s}^{-1}$ ) measured by ferrioxalate actinometry ( $\Phi = 1.26$ );<sup>41,42</sup>  $A$  = absorbance at 365 nm;  $dc/dt$  = initial rate of 4OHT release or Claisen product ( $\text{mol s}^{-1}$ ).<sup>42</sup>  
<sup>b</sup>Contribution from nonphotochemical (preexisting) hydrolysis excluded. nd = not detectable

compounds 7 or 8 show good stability in aqueous solution with no decomposition detected for either compound, at least during the entire incubation period of up to 24 h as determined by UPLC analysis.

The mechanism of 4OHT release by 5 involves photocleavage of the  $\text{CH}_2\text{-OC(=O)}$  bond followed by a loss of  $\text{CO}_2$  to yield free 4OHT (Figure 3). Similarly, both 7 and 8 rely on the same type of photocleavage reaction but instead yield release of 9, a 4OHT precursor. However, this derivative

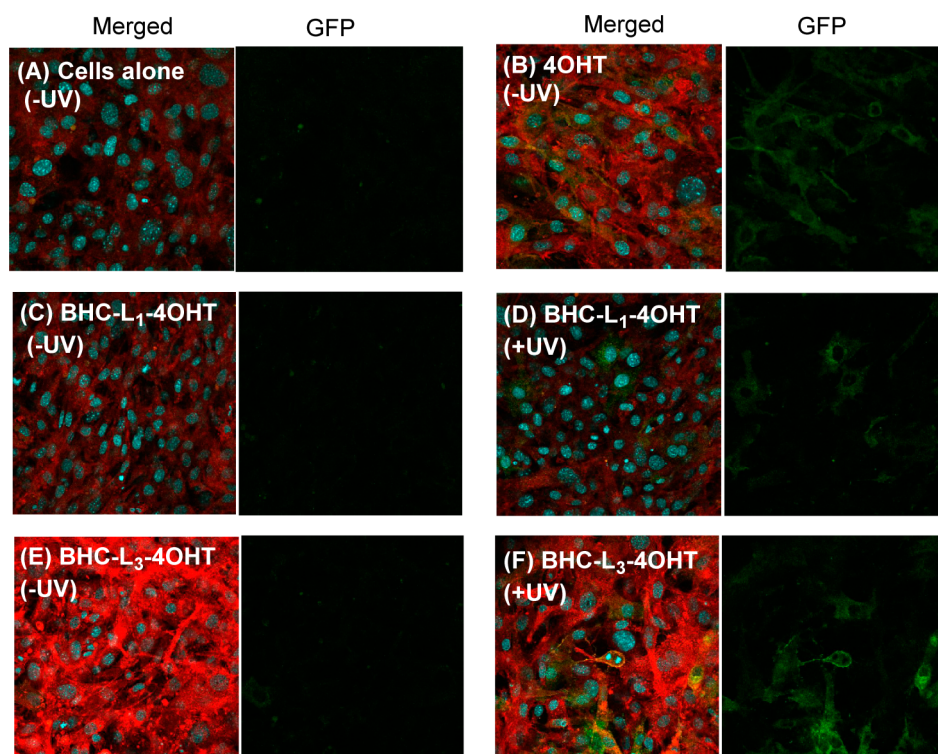


**Figure 5.** Confocal fluorescence microscopy analysis of the photocontrol of Cre-ERT2 mediated GFP expression in UbcCreERT2 mTmG MEF cells. As controls, MEFs were treated with (A) media alone or (B) 4OHT without UVA exposure. MEFs were treated with 2 BHC-L<sub>1</sub>-4OHT (C) without or (D) with UVA exposure. MEFs were treated with 7 BHC-L<sub>3</sub>-4OHT (E) without or (F) with UVA exposure. [4OHT or caged compound] = 250 nM. UVA exposure time = 3 min tdTomato fluorescence (red) and GFP fluorescence (green) are shown. Nuclei were labeled with DAPI (blue).

subsequently undergoes intramolecular self-immolation<sup>38,39</sup> through its spacer methyl(2-(methylamino)ethyl)carbamate<sup>25</sup> to release free 4OHT. Our observation that 7 shows both a greater decay rate and a higher quantum efficiency of 4OHT release than 8 (Table 1, Figure 4) clearly indicates that BHC in 7 is more effective in triggering the first photocleavage reaction than COM in 8.

**Cre-ERT2 Mediated GFP Expression *in Vitro*.** After validation of 4OHT release kinetics in solution, we selected two coumarin caged compounds 2 BHC-L<sub>1</sub>-4OHT and 7 BHC-L<sub>3</sub>-4OHT to compare their ability to control GFP expression in UbcCreERT2 mTmG MEF reporter cells (Figure 5). This cell line constitutively expresses Cre-ERT2 from the ubiquitin promoter and contains an mTmG reporter cassette which contains a loxP flanked gene for membrane bound red fluorescent protein (RFP), tdTomato.<sup>25,26</sup> TdTomato is constitutively expressed. However, upon Cre-ERT2 binding of free 4OHT, the loxP-flanked RFP gene is deleted by the translocated Cre recombinase, and a membrane bound GFP protein is expressed instead.

We first examined the photocontrol of the 4OHT constructs in the modulation of such switches in the expression of the reporter gene using confocal fluorescence microscopy. As similar to a published Protocol,<sup>25</sup> MEFs were treated with 4OHT, 2, or 7, each at a concentration of 250 nM in media and exposed to UVA light for 3 min, as this exposure time falls within the middle of the optimal exposure range for uncaging of all of the compounds tested (Figure 4). The cells were subsequently incubated at 37 °C for 24 h prior to being processed for confocal imaging. Cells treated with media alone and cells treated with each caged compound in the absence of

UVA exposure demonstrated a lack in detectable GFP fluorescence (Figure 5). Furthermore, untreated cells exposed to UVA for 3 min also showed no GFP fluorescence (Figure S14). In contrast, as a positive control, MEFs were treated with free 4OHT, which led to a detectable increase in GFP fluorescence even in the absence of UVA.

Cells treated with 2 or 7 with UVA exposure (+UVA; right) resulted in a substantial increase in GFP fluorescence intensity compared to the treated cells without UV exposure (left), validating UVA mediated photo-uncaging. However, GFP fluorescence induced by 2 appeared to be weaker than that induced by 7. While these differences between the activities of the two compounds as observed by confocal microscopy are only qualitative, these results are consistent with the release kinetics observed in solution where the release of free 4OHT upon UVA exposure was more efficient for 7 than for 2, the ether-linked compound that suffered from the photo-Claisen rearrangement as the major pathway for photocleavage. In contrast, a similar experiment with 5 BHC-L<sub>2</sub>-4OHT (±UVA) indicates its potent activity in inducing GFP expression, but with a lack of UV-mediated control (Figure S14), which is consistent with its hydrolytic instability in aqueous solutions (Figure S11). In summary, these confocal results are supportive of the ability of 4OHT caged compounds to control the induction of GFP expression through Cre-ERT2 recombinase activity in response to light. Our ongoing and future efforts are focused on developing and validating an efficient method of applying the probe 7 for spatiotemporal reporter activation *in vivo* as illustrated in Figure S15.

**Two-Photon Uncaging *in Vitro*.** After validation of release kinetics by single-photon exposure, we determined the

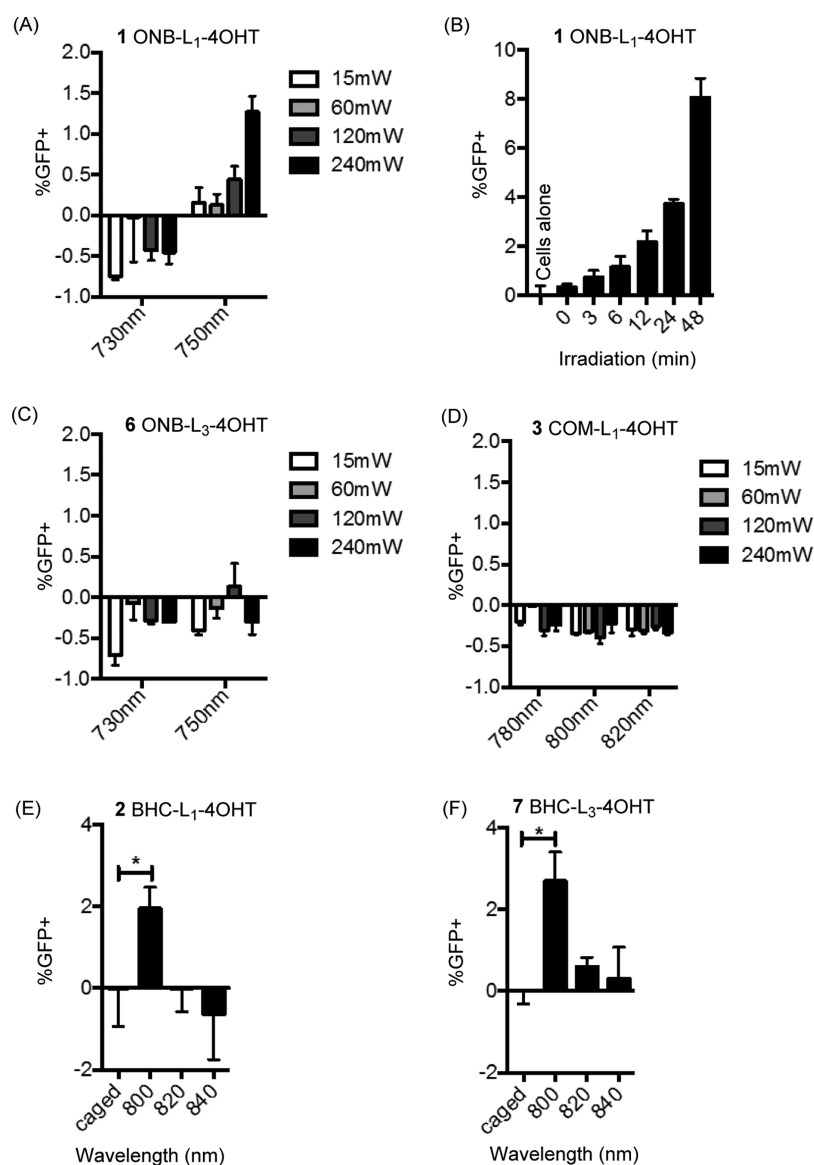


**Figure 6.** Two-photon activation of caged 4OHT compounds **1**, **2**, **3**, **6**, and **7**. (A, C, D) Hanging drops of **1**, **3**, and **6** were exposed to IR light for 10 min on the order of  $5 \times 10^{10}$  pulses (80 fs, 80 MHz) at different wavelengths at various powers. The uncaged compound solution was then diluted and added to UbcCre-ERT2 mTmG MEFs. At 24 h, the percent of GFP+ cells was determined by flow cytometry. Values of %GFP+ cells reported here refer to those obtained values after background correction by subtraction of the signal from cells exposed to a vehicle (DMSO) which was set to 0. (B) The above process was repeated with **1** for various irradiation times at 750 nm at 240 mW, and these were similarly used to convert reporter MEFs. The percent GFP+ cells was measured by flow cytometry. [**1**] = 100 nM, [**2**] = 2.5  $\mu$ M, [**3**] = 50 nM, [**6**] = 200 nM, [**7**] = 250 nM. \* $P < 0.05$ .

efficiency by which these compounds were uncaged by two-photon excitation (Figure 6). ONB groups have been reported to have narrow two-photon cross sections of absorption in the 750 nm range while coumarin (COM, BHC) cages have broader two-photon cross sections in the 800 nm range.<sup>6</sup> This means that coumarin cages uncage more efficiently at wavelengths more useful for use in tissue. As such we tested the uncaging efficiency of **1** ONB-L<sub>1</sub>-4OHT and **6** ONB-L<sub>3</sub>-4OHT by two-photon illumination at 730 and 750 nm, and **3** COM-L<sub>1</sub>-4OHT by two-photon illumination at each of three different wavelengths (780, 800, 820 nm) at various laser powers. To get significant uncaging ( $\geq 2\%$  GFP+) of **1**, 240 mW illumination was required at 750 nm for 10 min while % GFP+ was positively correlated with the irradiation time with a maximum value of  $\sim 8\%$  (Figure 6A,B). However, even at this

high power, **3** and **6** showed no appreciable uncaging (Figure 6C,D). The efficiency of uncaging of **1** could be improved by increasing the time of the exposure (Figure 6B); however at 240 mW, two-photon illumination using a pulsed laser at 750 nm would damage tissues which would be exacerbated by these long exposures. Compound **1** was more efficiently activated than **6** by two-photon illumination, consistent with the increased decay rate seen with single photon illumination.

Since **3** COM-L<sub>1</sub>-4OHT undergoes such a significant side reaction, it is likely this lack of uncaging is due to this inefficient uncaging. As such, we compared the efficiency of uncaging of BHC caged compounds **2** BHC-L<sub>1</sub>-4OHT and **7** BHC-L<sub>3</sub>-4OHT at wavelengths between 800 and 840 nm (Figure 6E,F). These uncaging experiments were performed at the concentration which is either identical to that used in Cre-ERT2



mediated GFP expression (250 nM for **7**; Figure 5) or higher (2.5  $\mu$ M for **2**) due to its relatively low efficiency of 4OHT release. Hanging drops of **2** and **7** were illuminated for 10 min at 120 mW laser power. Both **2** and **7** showed uncaging activity at 800 nm, and similar to the observations made for single-photon uncaging, **7** was also uncaged most efficiently by two-photon excitation. Indeed at 120 mW power for 10 min, **7** was 6 times more active in inducing GFP expression than **1** (2.7% GFP+ compared to 0.4% GFP+). The carbonate linked compound **5** was not tested for two photon uncaging as it is unstable in aqueous solutions and so was as potent at inducing GFP expression with or without UVA illumination (Figure S14).

**Conclusion.** In summary, we designed a series of new 4OHT probes caged with coumarin through the extended spacer for light controlled GFP gene expression in UbcCreERT2 mTmG MEFs and validated their effective uncaging activity *in vitro* by both single- and two-photon mechanisms. We believe that this study represents a significant advancement and gives new insights into the development of photoprobes that enable precise control of cell labeling based on a Cre-ER reporter system. Uncaging by single-photon irradiation occurred rapidly, in as short of an exposure time as 2 min for both BHC and COM caged compounds, with quantum efficiency ( $\Phi$ ) as high as 0.21 ( $\Phi$ , Table 1). BHC caged compounds exhibited more effective uncaging than their COM analogues. A representative compound, **7**, was activated on MEFs by UVA, demonstrating its ability to temporally induce GFP reporter expression.

Uncaging by two-photon irradiation induced an increase in the %GFP+ cells as high as 8% for certain caged compounds (Figure 6), though this was less efficient than that observed by single-photon irradiation (UVA).<sup>25</sup> This result was anticipated due to the generally lower efficiency of uncaging by two-photon.<sup>5,6</sup> The two-photon efficiency was dependent on the structural type of the cage, with BHC (**7**) showing greater GFP expression than ONB (**1**). Such higher efficiency by BHC is attributable primarily to its higher two-photon cross-section of absorption ( $\delta_{\text{absorption}}$ ) rather than its quantum efficiency of uncaging ( $\Phi = 0.21$ ), which is not significantly higher than that of ONB ( $\Phi = 0.13$ , Table 1). In addition, two-photon factors including irradiation wavelength, intensity, and exposure time made a significant contribution to the uncaging efficiency. However, due to the inability to have direct correlation between the two-photon and single-photon factors, systematic screening of these parameters for each compound was needed for the identification of the optimal uncaging conditions as done in this study.

We believe that this study offers rare insights into the mechanism of the photouncaging process and has broad implications in the field of photocaging technology. Despite the extensive use of coumarin caged compounds,<sup>3,6,37</sup> only few previous studies have indicated the occurrence of photorearrangement in caged thiols and phenols.<sup>31,34,37</sup> Our present study reports on the prevalence of photo-Claisen rearrangement<sup>33,36</sup> in coumarin ether caged compounds, but no evidence is observed for the implication of such rearrangement in ONB uncaging, which occurs exclusively *via* an intramolecular cyclization of its nitro group.<sup>6</sup> We attribute the basis of this photorearrangement to the radical-based mechanism of coumarin uncaging in combination with the presence of an ether linkage which, due to its shorter length in nature, brings the transient radical species generated by light exposure into

close proximity, thus promoting their recombination.<sup>33</sup> We suggest the incorporation of an extended linker as an effective strategy to circumvent its negative effect on uncaging efficiency. Use of this strategy enabled us to block this rearrangement possibly by sufficiently separating the two radical species within their solvent cages and thus preventing their recombination.

The photo-Claisen byproduct formed was not detectable by methods commonly used in this field such as UV-vis spectrometry (Figure 2B) or by TLC analysis, which had insufficient resolution of separation (Figure S7). Instead, its detection and quantitation required the development of a specific UPLC method that provides sufficient product resolution. Thus, this study highlights the importance of linker development in the design of 4OHT caged compounds, as well as in the design of other photocaged compounds, and underscores the importance of analytical method choice for evaluating the formed products. It is notable that a lack of such precise analysis can result in inaccurate interpretation of biological activities *in vitro* and *in vivo* as some of the byproduct-like C-4 substituted coumarin compounds are associated with promiscuous activities such as acting as ligands of estrogen receptors,<sup>43</sup> antioxidants,<sup>44</sup> and antiviral agents.<sup>45</sup>

## MATERIALS AND METHODS

Methods for the synthesis of caged 4OHT compounds and analytical methods (<sup>1</sup>H and <sup>13</sup>C NMR spectroscopy, UV-vis spectrometry, mass spectrometry, UPLC) are described in detail in the Supporting Information and the references cited therein. Full details for release kinetics<sup>25,26</sup> and cell studies *in vitro* (single-photon<sup>25</sup> and two-photon<sup>13</sup> uncaging for induction of GFP expression) are also provided in the Supporting Information.

## ASSOCIATED CONTENT

### Supporting Information

The Supporting Information is available free of charge on the ACS Publications website at DOI: 10.1021/acschembio.6b00999.

Methods for the synthesis of caged 4OHT compounds and analytical methods and full details for release kinetics and cell studies *in vitro* (PDF)

## AUTHOR INFORMATION

### Corresponding Authors

\*Phone: (415) 514-3130. E-mail: matthew.krummel@ucsf.edu.

\*Phone: (734) 647-0052. E-mail: skchoi@umich.edu.

### ORCID

Seok Ki Choi: 0000-0001-5633-4817

### Author Contributions

||These authors contributed equally.

### Notes

The authors declare no competing financial interest.

## ACKNOWLEDGMENTS

This work was supported in part by the National Cancer Institute, National Institutes of Health under award 1R21CA191428. SKC acknowledges support from Michigan Nanotechnology Institute for Medicine and Biological Sciences, University of Michigan Medical School.

## REFERENCES

(1) Billington, A. P., Walstrom, K. M., Ramesh, D., Guzikowski, A. P., Carpenter, B. K., and Hess, G. P. (1992) Synthesis and photo-

chemistry of photolabile N-glycine derivatives and effects of one on the glycine receptor. *Biochemistry* 31, 5500–5507.

(2) Lee, H.-M., Larson, D. R., and Lawrence, D. S. (2009) Illuminating the Chemistry of Life: Design, Synthesis, and Applications of "Caged" and Related Photoresponsive Compounds. *ACS Chem. Biol.* 4, 409–427.

(3) Brieke, C., Rohrbach, F., Gottschalk, A., Mayer, G., and Heckel, A. (2012) Light-Controlled Tools. *Angew. Chem., Int. Ed.* 51, 8446–8476.

(4) Yamazoe, S., Liu, Q., McQuade, L. E., Deiters, A., and Chen, J. K. (2014) Sequential Gene Silencing Using Wavelength-Selective Caged Morpholino Oligonucleotides. *Angew. Chem., Int. Ed.* 53, 10114–10118.

(5) Hansen, M. J., Velema, W. A., Lerch, M. M., Szymanski, W., and Feringa, B. L. (2015) Wavelength-selective cleavage of photo-protecting groups: strategies and applications in dynamic systems. *Chem. Soc. Rev.* 44, 3358–3377.

(6) Klán, P., Šolomek, T., Bochet, C. G., Blanc, A., Givens, R., Rubina, M., Popik, V., Kostikov, A., and Wirz, J. (2012) Photo-removable Protecting Groups in Chemistry and Biology: Reaction Mechanisms and Efficacy. *Chem. Rev. (Washington, DC, U. S.)* 113, 119–191.

(7) Goguen, B. N., Aemissegger, A., and Imperiali, B. (2011) Sequential Activation and Deactivation of Protein Function Using Spectrally Differentiated Caged Phosphoamino Acids. *J. Am. Chem. Soc.* 133, 11038–11041.

(8) Wong, P. T., Tang, S., Cannon, J., Mukherjee, J., Isham, D., Gam, K., Payne, M., Yanik, S. A., Baker, J. R., and Choi, S. K. (2017) A Thioacetal Photocage Designed for Dual Release: Application in the Quantitation of Therapeutic Release by Synchronous Reporter Decaging. *ChemBioChem* 18, 126–135.

(9) Furuta, T., Wang, S. S. H., Dantzker, J. L., Dore, T. M., Bybee, W. J., Callaway, E. M., Denk, W., and Tsien, R. Y. (1999) Brominated 7-hydroxycoumarin-4-ylmethyls: Photolabile protecting groups with biologically useful cross-sections for two photon photolysis. *Proc. Natl. Acad. Sci. U. S. A.* 96, 1193–1200.

(10) Givens, R. S., Rubina, M., and Wirz, J. (2012) Applications of p-hydroxyphenacyl (pHP) and coumarin-4-ylmethyl photoremovable protecting groups. *Photochem. Photobiol. Sci.* 11, 472–488.

(11) Momotake, A., Lindegger, N., Niggli, E., Barsotti, R. J., and Ellis-Davies, G. C. R. (2006) The nitrodibenzofuran chromophore: a new caging group for ultra-efficient photolysis in living cells. *Nat. Methods* 3, 35–40.

(12) Li, Y. M., Shi, J., Cai, R., Chen, X., Luo, Z. F., and Guo, Q. X. (2010) New quinoline-based caging groups synthesized for photo-regulation of aptamer activity. *J. Photochem. Photobiol., A* 211, 129–134.

(13) Pettit, D. L., Wang, S. S. H., Gee, K. R., and Augustine, G. J. (1997) Chemical Two-Photon Uncaging: a Novel Approach to Mapping Glutamate Receptors. *Neuron* 19, 465–471.

(14) Lemke, E. A., Summerer, D., Geierstanger, B. H., Brittain, S. M., and Schultz, P. G. (2007) Control of protein phosphorylation with a genetically encoded photocaged amino acid. *Nat. Chem. Biol.* 3, 769–772.

(15) Karginov, A. V., Zou, Y., Shirvanyants, D., Kota, P., Dokholyan, N. V., Young, D. D., Hahn, K. M., and Deiters, A. (2010) Light Regulation of Protein Dimerization and Kinase Activity in Living Cells Using Photocaged Rapamycin and Engineered FKBP. *J. Am. Chem. Soc.* 133, 420–423.

(16) Ceo, L. M., and Koh, J. T. (2012) Photocaged DNA Provides New Levels of Transcription Control. *ChemBioChem* 13, 511–513.

(17) Lerch, M. M., Hansen, M. J., van Dam, G. M., Szymanski, W., and Feringa, B. L. (2016) Emerging Targets in Photopharmacology. *Angew. Chem., Int. Ed.* 55, 10978–10999.

(18) Velema, W. A., van der Berg, J. P., Szymanski, W., Driessen, A. J. M., and Feringa, B. L. (2014) Orthogonal Control of Antibacterial Activity with Light. *ACS Chem. Biol.* 9, 1969–1974.

(19) Wong, P. T., Chen, D., Tang, S., Yanik, S., Payne, M., Mukherjee, J., Coulter, A., Tang, K., Tao, K., Sun, K., Baker, J. R., Jr,

and Choi, S. K. (2015) Modular Integration of Upconversion Nanocrystal-Dendrimer Composites for Folate Receptor-Specific Near Infrared Imaging and Light Triggered Drug Release. *Small* 11, 6078–6090.

(20) Yang, Y., Shao, Q., Deng, R., Wang, C., Teng, X., Cheng, K., Cheng, Z., Huang, L., Liu, Z., Liu, X., and Xing, B. (2012) In Vitro and In Vivo Uncaging and Bioluminescence Imaging by Using Photocaged Upconversion Nanoparticles. *Angew. Chem., Int. Ed.* 51, 3125–3129.

(21) Agasti, S. S., Laughney, A. M., Kohler, R. H., and Weissleder, R. (2013) A photoactivatable drug-caged fluorophore conjugate allows direct quantification of intracellular drug transport. *Chem. Commun. (Cambridge, U. K.)* 49, 11050–11052.

(22) Link, K. H., Shi, Y., and Koh, J. T. (2005) Light Activated Recombination. *J. Am. Chem. Soc.* 127, 13088–13089.

(23) Lu, X., Agasti, S. S., Vinegoni, C., Waterman, P., DePinho, R. A., and Weissleder, R. (2012) Optochemogenetics (OCG) Allows More Precise Control of Genetic Engineering in Mice with CreER regulators. *Bioconjugate Chem.* 23, 1945–1951.

(24) Sinha, D. K., Neveu, P., Gagey, N., Aujard, I., Benbrahim-Bouzidi, C., Le Saux, T., Rampon, C., Gauron, C., Goetz, B., Dubruille, S., Baaden, M., Volovitch, M., Bensimon, D., Vriza, S., and Jullien, L. (2010) Photocontrol of Protein Activity in Cultured Cells and Zebrafish with One- and Two-Photon Illumination. *ChemBioChem* 11, 653–663.

(25) Faal, T., Wong, P., Tang, S., Coulter, A., Chen, Y., Tu, C. H., Baker, J. R., Choi, S. K., and Inlay, M. A. (2015) 4-Hydroxytamoxifen probes for light-dependent spatiotemporal control of Cre-ER mediated reporter gene expression. *Mol. Biosyst.* 11, 783–790.

(26) Inlay, M. A., Choe, V., Bharathi, S., Fernhoff, N. B., Baker, J. R., Weissman, I. L., and Choi, S. K. (2013) Synthesis of a photocaged tamoxifen for light-dependent activation of Cre-ER recombinase-driven gene modification. *Chem. Commun. (Cambridge, U. K.)* 49, 4971–4973.

(27) Shi, Y., and Koh, J. T. (2004) Light-Activated Transcription and Repression by Using Photocaged SERMs. *ChemBioChem* 5, 788–796.

(28) Madisen, L., Mao, T., Koch, H., Zhuo, J.-m., Berenyi, A., Fujisawa, S., Hsu, Y.-W. A., Garcia, A. J., Gu, X., Zanello, S., Kidney, J., Gu, H., Mao, Y., Hooks, B. M., Boyden, E. S., Buzsaki, G., Ramirez, J. M., Jones, A. R., Svoboda, K., Han, X., Turner, E. E., and Zeng, H. (2012) A toolbox of Cre-dependent optogenetic transgenic mice for light-induced activation and silencing. *Nat. Neurosci.* 15, 793–802.

(29) Muzumdar, M. D., Tasic, B., Miyamichi, K., Li, L., and Luo, L. (2007) A global double-fluorescent Cre reporter mouse. *Genesis* 45, 593–605.

(30) Ruzankina, Y., Pinzon-Guzman, C., Asare, A., Ong, T., Pontano, L., Cotsarelis, G., Zediak, V. P., Velez, M., Bhandoola, A., and Brown, E. J. (2007) Deletion of the Developmentally Essential Gene ATR in Adult Mice Leads to Age-Related Phenotypes and Stem Cell Loss. *Cell Stem Cell* 1, 113–126.

(31) Kotzur, N., Briand, B., Beyersmann, M., and Hagen, V. (2009) Wavelength-Selective Photoactivatable Protecting Groups for Thiols. *J. Am. Chem. Soc.* 131, 16927–16931.

(32) San Miguel, V., Bochet, C. G., and del Campo, A. (2011) Wavelength-Selective Caged Surfaces: How Many Functional Levels Are Possible? *J. Am. Chem. Soc.* 133, 5380–5388.

(33) Galindo, F. (2005) The photochemical rearrangement of aromatic ethers: A review of the Photo-Claisen reaction. *J. Photochem. Photobiol., C* 6, 123–138.

(34) Schaal, J., Kotzur, N., Dekowski, B., Quilitz, J., Klimakow, M., Wessig, P., and Hagen, V. (2009) A novel photorearrangement of (coumarin-4-yl)methyl phenyl ethers. *J. Photochem. Photobiol., A* 208, 171–179.

(35) Kim, S., Kang, D., Lee, C.-H., and Lee, P. H. (2012) Synthesis of Substituted Coumarins via Brønsted Acid Mediated Condensation of Allenes with Substituted Phenols or Anisoles. *J. Org. Chem.* 77, 6530–6537.

(36) Pincock, A. L., Pincock, J. A., and Stefanova, R. (2002) Substituent Effects on the Rate Constants for the Photo-Claisen Rearrangement of Allyl Aryl Ethers. *J. Am. Chem. Soc.* 124, 9768–9778.

(37) Mahmoodi, M. M., Abate-Pella, D., Pundsack, T. J., Palsuledesai, C. C., Goff, P. C., Blank, D. A., and Distefano, M. D. (2016) Nitrodibenzofuran: A One- and Two-Photon Sensitive Protecting Group That Is Superior to Brominated Hydroxycoumarin for Thiol Caging in Peptides. *J. Am. Chem. Soc.* 138, 5848–5859.

(38) Amir, R. J., Pessah, N., Shamis, M., and Shabat, D. (2003) Self-Immolative Dendrimers. *Angew. Chem., Int. Ed.* 42, 4494–4499.

(39) Steiger, A. K., Pardue, S., Kevil, C. G., and Pluth, M. D. (2016) Self-Immolative Thiocarbamates Provide Access to Triggered H<sub>2</sub>S Donors and Analyte Replacement Fluorescent Probes. *J. Am. Chem. Soc.* 138, 7256–7259.

(40) Kim, Y. A., Ramirez, D. M. C., Costain, W. J., Johnston, L. J., and Bittman, R. (2011) A new tool to assess ceramide bioactivity: 6-bromo-7-hydroxycoumarinyl-caged ceramide. *Chem. Commun. (Cambridge, U. K.)* 47, 9236–9238.

(41) Hatchard, C. G., and Parker, C. A. (1956) A New Sensitive Chemical Actinometer. II. Potassium Ferrioxalate as a Standard Chemical Actinometer. *Proc. R. Soc. London, Ser. A* 235, 518–536.

(42) Braslavsky, S. E. (2009) Glossary of terms used in photochemistry, 3rd edition (IUPAC Recommendations 2006). *Pure Appl. Chem.* 79, 293–465.

(43) Kirkiacharian, S., Lormier, A. T., Chidiack, H., Bouchoux, F., and C er ede, E. (2004) Synthesis and binding affinity to human  $\alpha$  and  $\beta$  estrogen receptors of various 7-hydroxycoumarins substituted at 4- and 3,4- positions. *Farmaco* 59, 981–986.

(44) Raj, H. G., Parmar, V. S., Jain, S. C., Goel, S., Himanshu, P., Malhotra, S., Singh, A., Olsen, C. E., and Wengel, J. (1998) Mechanism of Biochemical Action of Substituted 4-Methylbenzopyran-2-ones. Part I: Dioxygenated 4-Methyl Coumarins as Superb Antioxidant and Radical Scavenging Agents. *Bioorg. Med. Chem.* 6, 833–839.

(45) Hassan, M. Z., Osman, H., Ali, M. A., and Ahsan, M. J. (2016) Therapeutic potential of coumarins as antiviral agents. *Eur. J. Med. Chem.* 123, 236–255.